Electronic Supplementary Information

Keggin-type polyoxometalate nanosheets: Synthesis and characterization via scanning transmission electron microscopy

Norihito Hiyoshi

Research Institute for Chemical Process Technology,
National Institute of Advanced Industrial Science and Technology (AIST),
4-2-1 Nigatake, Miyagino, Sendai 983-8551, Japan
E-mail: n-hiyoshi@aist.go.jp

Table of Contents

1. Experimental

1-1. Materials

Silicotungstic acid hydrate (383341, Sigma-Aldrich Co. LLC.), cesium chloride (Wako Pure Chemical Industries, Ltd.), hydrochloric acid (Wako Pure Chemical Industries, Ltd.) and *n*-octylamine (Wako Pure Chemical Industries, Ltd.) were used as received. Light curing embedding resin (LCR D-800, Toagosei Co., Ltd.) was purchased from JEOL Ltd.. Quantifoil® support foils (Quantifoil Micro Tools GmbH) were purchased from EM Japan Co., Ltd..

1-2. Preparation of POM nanosheet

Preparation of the POM nanosheets was conducted by mixing an aqueous solution of silicotungstic acid (1.5 mmol·dm^{-3}, 20 cm^3) and an aqueous solution (10 cm^3) containing cesium chloride (3.0 mmol·dm^{-3}), *n*-octylamine (2.1 mmol·dm^{-3}), and hydrochloric acid (0.1 mol·dm^{-3}). The solution was transferred to a Petri dish (60 mm inner diameter) with a lid and left to stand for 16 h at 293 K.

1-3. Characterization

The products were observed via optical microscopy and STEM. The reflected bright field image of the solution surface (Figure S4) was obtained with a BM-3400TTRL optical microscope (Wraymer Inc.). The phase contrast image (Figure 1a) was obtained with a CKX53 optical microscope (Olympus Co.) equipped with an LUCPLFLN20XPH objective lens (Olympus Co.). The optical microscopy images were recorded with a WRAYCAM-NF300 CMOS camera (Wraymer Inc.). The STEM observation was preformed using an ARM-200F electron microscope (JEOL Ltd.) equipped with a CEOS aberration corrector (Corrected Electron Optical Systems GmbH). The electron microscope was operated at an accelerating voltage of 200 kV, and the STEM images were recorded with annular dark field (ADF) detectors (JEOL Ltd.). The EDS analysis was performed with a 100 mm^2 silicon drift detector (JEOL Ltd.) equipped for the electron microscope. Sample preparation methods and observation conditions are shown in Figures S1–S3 and Table S1.

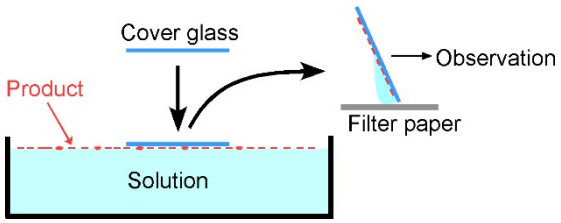

Figure S1. Sample preparation procedure for phase contrast observation (Figure 1a).

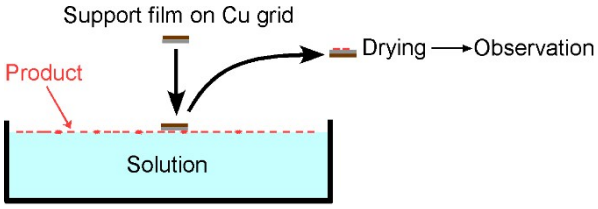

Figure S2. Sample preparation procedure for STEM observation (Figures 1b, 3a, 3c, 3d, 4).

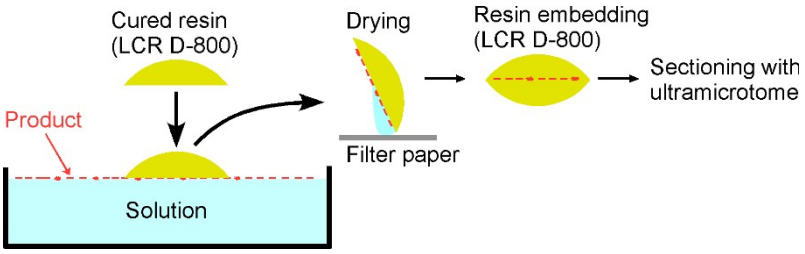

Figure S3. Sample preparation procedure for cross-section observation (Figures 1c, 2a, 2b).

Table S1. Support film used for STEM sample preparation, collection angle of ADF detector [a], and image processing method.

Image	Support film	Collection semi-angle /mrad	Image processing method
Figures 1b, S6	Quantifoil® R0.6/1	45–175	–
Figure 1c	Quantifoil® Multi	45–175	–
Figure 2a	Quantifoil® Multi	45–175	Smoothing
Figure 2b	Quantifoil® Multi	45–175	Smoothing
Figures 3a, 3c	Carbon film (<5 nm) on Quantifoil®	45–175	3a: Local-2D Wiener Filter [b] 3c: Smoothing
Figure 3d	Carbon film (<5 nm) on Quantifoil®	20–80	Local-2D Wiener Filter [b]
Figures 4, S7	Carbon film (<5 nm) on Quantifoil®	20–80	4: Local-2D Wiener Filter [b] S7: Smoothing
Figure 5a	Quantifoil® R0.6/1	45–175	Smoothing

[a] The convergence semi-angle was 14 mrad. [b] In HREM-Filters Pro software (HREM Research Inc.)

2. Structures of Keggin anion and salt composed of Keggin anions and alkali metal cations

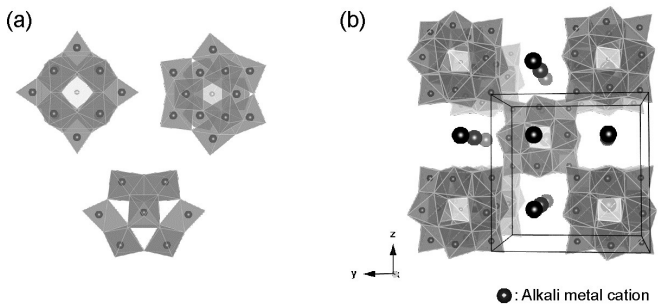

Figure S4. (a) Structure of Keggin anion viewed along various directions. (b) Cubic crystal structure of salt composed of Keggin anions and alkali metal cations.

3. Reflected bright field image of solution surface

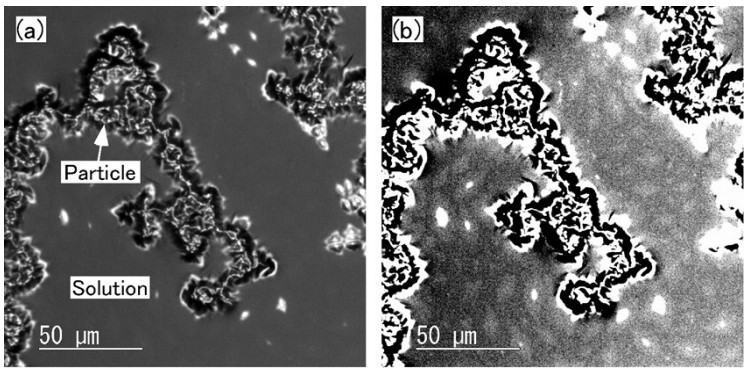

Figure S5. (a) Optical micrograph (reflected bright field image) of surface of solution containing silicotungstic acid, cesium chloride, *n*-octylamine, and hydrochloric acid after 16 h. (b) Contrast of (a) was enhanced.

4. Line profile of STEM image of Figure 1b

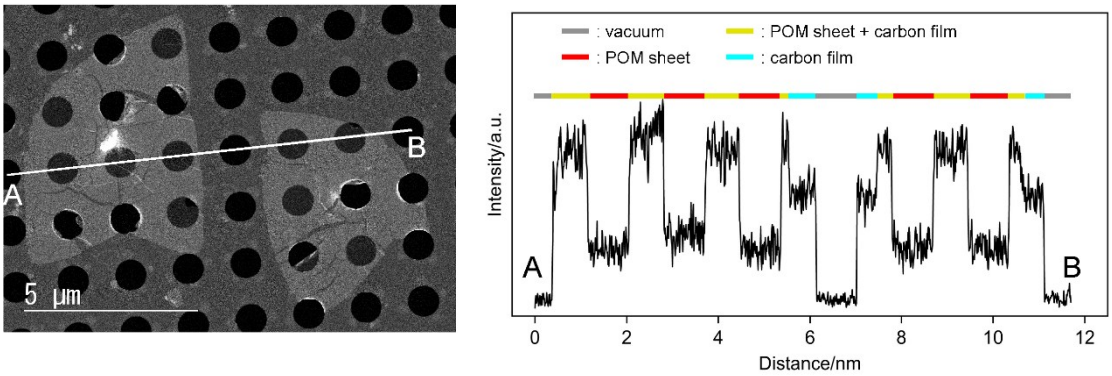

Figure S6. Line profile of STEM image (Fig. 1(b)) between point A and point B.

5. Line profile of STEM image of Figure 4

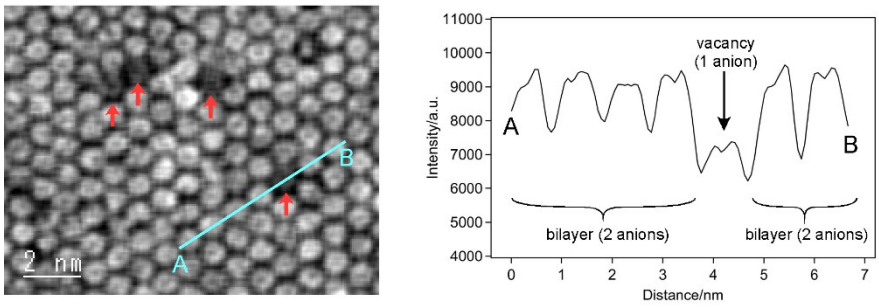

Figure S7. Smoothed STEM image of POM nanosheet obtained along [111] direction and line profile between point A and point B. Arrows indicate anion vacancies.

6. EDS analysis of layered particle

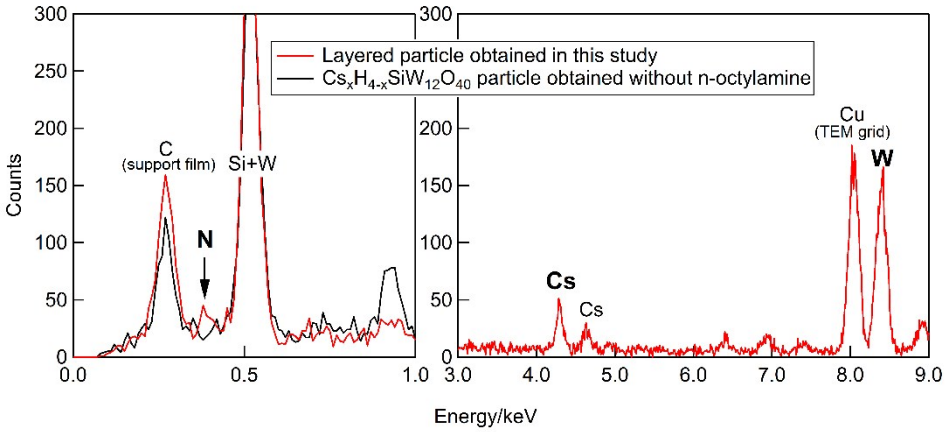

Figure S8. EDS spectra of layered particle obtained in this study and $Cs_xH_{4-x}SiW_{12}O_{40}$ particle obtained without *n*-octylamine.

From the EDS spectrum of the layered particle, the ratios of *n*-octylamine and Cs^+ to $[SiW_{12}O_{40}]^{4-}$ were roughly estimated to be three and 2.4, respectively. If protonated *n*-octylamine molecules and cesium cations occupy the outside and inside cation sites of the layers, respectively, the ideal composition is $(C_8H_{20}N)_2Cs_2SiW_{12}O_{40}$. The result of EDS analysis suggests that the layered particles have this structure.

7. Thermal stability of nanosheets

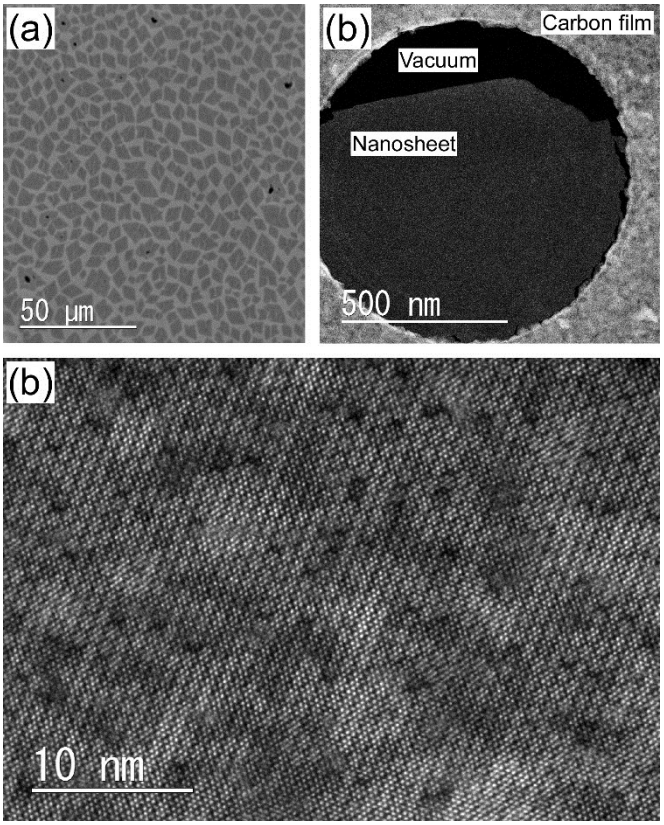

Figure S9. (a) Optical micrograph (phase contrast image) of POM nanosheets on cover glass after heat treatment up to 573 K in air, (b) STEM image of POM nanosheet on carbon support film after heat treatment up to 573 K under vacuum (c) High-resolution STEM image of POM nanosheet on carbon support film after heat treatment up to 573 K under vacuum.

Figure S9a shows an optical micrograph image of the nanosheets which were loaded on a cover glass and heated in air up to 573 K. The optical micrograph image shows that the morphology of the nanosheets are not changed after the heat treatment. In addition, Figures S9b and S9c, which show STEM images of the nanosheets heated under vacuum up to 573 K, indicate that the crystal structure is not changed after the heat treatment. These results demonstrate that the nanosheets are thermally stable up to 573 K.

8. XRD patterns of products (nanosheets and layered particle) on cover glass

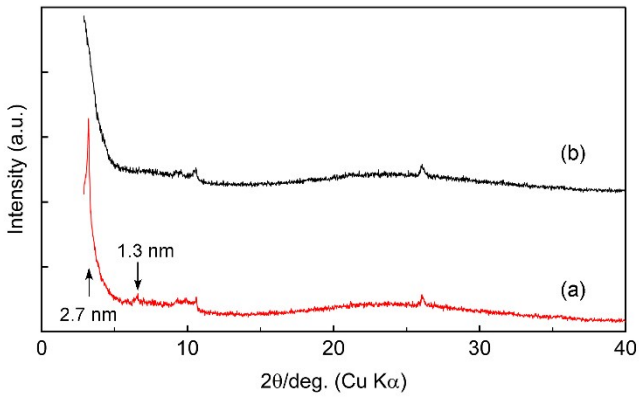

Figure S10. (a) XRD pattern of products formed of solution surface and loaded on cover glass, (b) XRD pattern after heat treatment of (a) up to 573 K in air.

In the XRD pattern of products loaded on a cover glass (pattern a), a diffraction peak at 2θ = 3.22° (d = 2.7 nm) and its second-order peak at 2θ = 6.60° (d = 1.3 nm) are observed. The *d* values of these peaks correspond to the inter-layer distance of the layered particles (2.5 nm) shown in Figure 5a. The peaks due to the layered structure (3.22 and 6.60°) are disappeared after the heat treatment at 573 K in air (pattern b). These results indicate that the amounts of *n*-octylamine molecules in the interlayer spaces are reduced by the heat treatment. Furthermore, this result strongly suggests that *n*-octylamine molecules attaching to the nanosheets can be also desorbed and/or decomposed by the heat treatment.

9. Raw image data

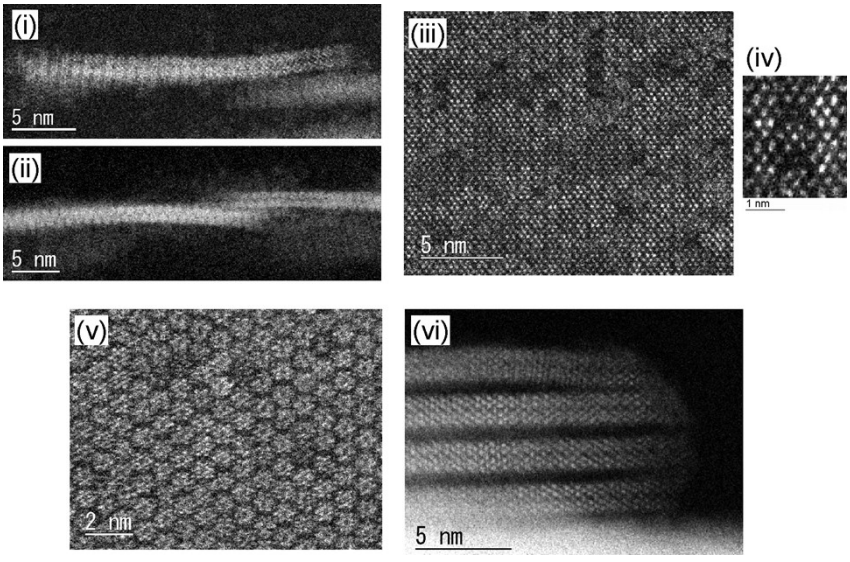

Figure S9. Raw image data of (i) Figure 2a, (ii) Figure 2b, (iii) Figures 3a and 3c, (iv) Figure 3d, (v) Figures 4 and S7, and (vi) Figure 5a.